J|A|C|S
ARTICLES
Published on Web 01/24/2002

The Nature of the Intermediates in the Reactions of Fe(III)- and Mn(III)-Microperoxidase-8 with H_2O_2: a Rapid Kinetics Study

Jean-Louis Primus,[†,||,⊥] Sylvie Grunenwald,[‡] Peter-Leon Hagedoorn,[§] Anne-Marie Albrecht-Gary,[‡] Dominique Mandon,[||] and Cees Veeger*[,†]

Contribution from the Laboratory of Biochemistry, Wageningen University, Dreijenlaan 3, 6703 HA Wageningen, The Netherlands, Laboratoire de Physico-Chimie Bioinorganique, UMR 7509, Université Louis Pasteur, 1, rue Blaise Pascal, 67000 Strasbourg, France, Kluyver Department of Biotechnology, Delft University of Technology, Julianalaan 67, 2628 BC Delft, The Netherlands, and Laboratoire de Cristallochimie, UMR 7513, Université Louis Pasteur, 4, rue Blaise Pascal, 67070 Strasbourg, France

Received August 21, 2001. Revised Manuscript Received November 8, 2001

Abstract: Kinetic studies were performed with microperoxidase-8 (Fe(III)MP-8), the proteolytic breakdown product of horse heart cytochrome *c* containing an octapeptide linked to an iron protoporphyrin IX. Mn(III) was substituted for Fe(III) in Mn(III)MP-8.The mechanism of formation of the reactive metal-oxo and metal-hydroperoxo intermediates of M(III)MP-8 upon reaction of H_2O_2 with Fe(III)MP-8 and Mn(III)MP-8 was investigated by rapid-scan stopped-flow spectroscopy and transient EPR. Two steps (k_{obs1} and k_{obs2}) were observed and analyzed for the reaction of hydrogen peroxide with both catalysts. The plots of k_{obs1} as function of $[H_2O_2]$ at pH 8.0 and pH 9.1 for Fe(III)MP-8, and at pH 10.2 and pH 10.9 for Mn(III)MP-8, exhibit saturation kinetics, which reveal the accumulation of an intermediate. Double reciprocal plots of $1/k_{obs1}$ as function of $1/[H_2O_2]$ at different pH values reveal a competitive effect of protons in the oxidation of M(III)MP-8. This effect of protons is confirmed by the linear dependence of $1/k_{obs1}$ on $[H^+]$ showing that k_{obs1} increases with the pH. The UV−visible spectra of the intermediates formed at the end of the first step (k_{obs1}) exhibit a spectrum characteristic of a high-valent metal-oxo intermediate for both catalysts. Transient EPR of Mn(III)MP-8 incubated with an excess of H_2O_2, at pH 11.5, shows the detection of a free radical signal at $g \approx 2$ and of a resonance at $g \approx 4$ characteristic of a Mn(IV) ($S = 3/2$) species. On the basis of these results, the following mechanism is proposed: (i) M(III)MP-8-OH_2 is deprotonated to M(III)MP-8-OH in a rapid preequilibrium step, with a $pK_a = 9.2 \pm 0.9$ for Fe(III)MP-8 and a $pK_a = 11.2 \pm 0.3$ for Mn(III)-MP-8; (ii) M(III)MP-8-OH reacts with H_2O_2 to form Compound 0, M(III)MP8-OOH, with a second-order rate constant $k_1 = (1.3 \pm 0.6) \times 10^6$ $M^{-1}\cdot s^{-1}$ for Fe(III)MP-8 and $k_1 = (1.6 \pm 0.9) \times 10^5$ $M^{-1}\cdot s^{-1}$ for Mn(III)-MP-8; (iii) this metal-hydroperoxo intermediate is subsequently converted to a high-valent metal-oxo species, M(IV)MP-8=O, with a free radical on the peptide ($R^{\bullet+}$). The first-order rate constants for the cleavage of the hydroperoxo group are $k_2 = 165 \pm 8$ s^{-1} for Fe(III)MP-8 and $k_2 = 145 \pm 7$ s^{-1} for Mn(III)MP-8; and (iv) the proposed M(IV)MP-8=O($R^{\bullet+}$) intermediate slowly decays (k_{obs2}) with a rate constant of $k_{obs2} = 13.1 \pm 1.1$ s^{-1} for Fe(III)MP-8 and $k_{obs2} = 5.2 \pm 1.2$ s^{-1} for Mn(III)MP-8. The results show that Compound 0 is formed *prior* to what is analyzed as a high-valent metal-oxo peptide radical intermediate.

Introduction

Protons play a fundamental role in the formation of the catalytic reactive species for both peroxidases and cytochromes P450 (P450s). But, whereas the influence of protons in the distal heme active site starts to be better understood for peroxidases such as horseradish peroxidase (HRP),[1a,b] it remains less well defined for P450s.[2] Reactivity studies have shown that residues of the heme distal active site of peroxidases act as acid/base catalysts to facilitate the deprotonation of the hydroperoxide substrate and the subsequent heterolytic cleavage of the O−O peroxide bond.[3a,b,c] This leads to the formation of peroxidase Compound I, a high-valent iron-oxo porphyrin radical cation, $Por^{\bullet+}Fe(IV)=O$,[4a,b,c] which upon reduction by substrate is converted into peroxidase Compound II, PorFe(IV)=O.[5a,b] The porphyrin iron-hydroperoxo, PorFe(III)-OOH or Compound 0,

* To whom correspondence should be addressed. Phone: 31-(0)317-482 868. Fax: 31-(0)317-484 801. E-mail: cees.veeger@planet.nl.
† Laboratory of Biochemistry, Wageningen University.
‡ Laboratoire de Physico-Chimie Bioinorganique, Université Louis Pasteur.
§ Kluyver Department of Biotechnology, Delft University of Technology.
|| Laboratoire de Cristallochimie, Université Louis Pasteur.
⊥ Present address: IMEC, Kapeldreef 75, B-3001 Heverlee, Belgium.

(1) (a) Mukai, M.; Nagano, S.; Tanaka, M.; Ishimori, K.; Morishima, I.; Ogura, T.; Watanabe, Y.; Kitagawa, T. *J. Am. Chem. Soc.* **1997**, *119*, 1758−1766. (b) Banci, L. *J. Biotechnol.* **1997**, *53*, 253−263.
(2) Poulos, T. L.; Raag, R. *FASEB J.* **1992**, *6*, 674−679.
(3) (a) Ortiz de Montellano, P. R. *Annu. Rev. Pharmacol. Toxicol.* **1992**, *32*, 89−107. (b) Savenkova, M. I.; Kuo, J. M.; Ortiz de Montellano, P. R. *Biochemistry* **1998**, *37*, 10828−10836. (c) Smith, A. T.; Veitch, N. *Curr. Opin. Chem. Biol.* **1998**, *2*, 269−278.

10.1021/ja016907u CCC: $22.00

was detected for HRP[6a,b] at low temperature in 50% MeOH, in the presence of a high concentration of hydroperoxide. Also, the transient formation of a porphyrin iron-hydroperoxo was detected for the Arg38Leu HRP mutant;[7] Arg38 is proposed to be part of the proton-binding network in horseradish peroxidase. Indirect evidence for the existence of PorFe(III)-OOH in the reaction cycle of HRP comes from ^{18}O-exchange studies.[8a,b] Compound 0 and its deprotonated form, PorFe(III)-O−O$^-$ are species encountered in the P450 chemistry and precede an isoelectronic analogue of peroxidase Compound I in the reaction cycle.[9]

The comprehension of the acid/base catalysis and the formation of the high-valent iron-oxo or of the iron-peroxo intermediates for peroxidase and P450 chemistry has benefited from the use of synthetic metalloporphyrin models.[10a,b,c,d] Non μ-oxo dimer forming water-soluble model porphyrins such as FeTDCPPS and MnTDCPPS were used to study the influence of the pH on the formation of manganese- and iron-hydroperoxo intermediates and on the formation of high-valent manganese- and iron-oxo intermediates.[11a,b,c] However, these models all lack an anchored proximal ligand, even though studies were performed in the presence of free imidazole to mimic the proximal histidine ligand.[11c,12] The influence of this proximal ligand is an important parameter to consider in the formation of reactive intermediates in oxidation catalysis. Microperoxidase-8, Fe(III)-MP-8, is a water-soluble biomimic consisting of an iron protoporphyrin IX covalently attached to an octapeptide via two thioether bonds and one axial coordination bond between the iron and the histidine 18 residue of the peptide. Fe(III)MP-8 is obtained by controlled proteolytic digestion of horse heart cytochrome *c* and corresponds to residues 14−21 of the parent protein.[13] The fact that Fe(III)MP-8 can be used as a model for both peroxidase chemistry and P450 chemistry[13,14] makes it an attractive mimic for studying the influence of the pH on the formation of iron-(hydro)peroxo and high-valent iron-oxo intermediates. Several studies on possible reactive heme-oxygen species formed by microperoxidase biomimics exist.[15−19] The manganese complex of MP-8 was prepared to compare its reactivity with the iron complex of MP-8[15] and catalytic studies pointed at the involvement of Compound 0 in MP-8-catalyzed oxygen transfer reactions.[16] Stopped-flow kinetic studies performed on Fe(III)MP-11 in the presence of H_2O_2 at pH 7 and pH 10.4 showed the formation of a species tentatively assigned to peroxidase Compound I.[17] Investigations by UV−visible spectroscopy on Fe(III)MP-8 oxidized by photoinduced single-electron transfer showed the formation of an iron-hydroxo porphyrin radical cation, Por$^{\bullet+}$Fe(III)MP-8-OH, converting into peroxidase Compound II, PorFe(IV)MP-8=O, when the pH was increased.[18] Oxidation of Mn(III)MP-8 by H_2O_2 showed the formation of a manganese MP-8 analogue of peroxidase Compound II, Mn(IV)MP-8=O, characterized by UV−visible and Raman spectroscopy.[15] Low-temperature stopped-flow kinetic studies performed in 50% MeOH on N−Acetyl-Fe(III)-MP-8 in the presence of H_2O_2 have postulated the formation of Fe(III)MP-8-OOH *prior* to the formation of a putative Fe(III)-MP-8 peroxidase Compound I and Compound II.[19a] However, MeOH is a chaotropic and reducing agent, and moreover, it reacts with H_2O_2-produced intermediates of Fe(III)MP-8.[19b]

The goal of the present work was to study the oxidation chemistry of Fe(III)MP-8 and Mn(III)MP-8 in water at ambient temperature with particular attention to the role played by protons in the formation of iron-hydroperoxo and high-valent iron-oxo intermediates. The reactivity of Fe(III)MP-8 with H_2O_2 is compared to the reactivity of Mn(III)MP-8 with H_2O_2 using rapid kinetics and rapid-freeze EPR. The influence of the nature of the axial sixth ligand, aquo or hydroxo, on the formation of iron- or manganese-(hydro)peroxo intermediates is investigated. The consequences, for the formation and for the nature, of the high-valent iron- or manganese-oxo intermediates, are studied.

Results

The rate of formation of the oxidized intermediates of Fe(III)-MP-8 and Mn(III)MP-8 upon reaction with H_2O_2 were analyzed within the pH range corresponding to the optimal activity of Fe(III)MP-8 ($8 < pH < 10$) and Mn(III)MP-8 ($10 < pH < 13$) for peroxidase- and P450-type of conversions.[16] The time-dependent changes in the UV−visible spectrum of both catalysts upon oxidation by H_2O_2 are depicted in Figure 1a for Fe(III)-MP-8 and in Figure 1b for Mn(III)MP-8. A sample of the recorded transient traces at 410 nm for Fe(III)MP-8 incubated at pH 9.1 and at 400 nm for Mn(III)MP-8 incubated at pH 10.9 is depicted in the inset of Figure 1a and 1b, respectively. The transient traces obtained under varying pH and [H_2O_2] conditions were observed and analyzed using a biexponential fitting of the absorbance changes with time. Subsequent degradation steps of the catalysts were not considered in the present study. The variations of the pseudo-first-order rate constant k_{obs1} for Fe(III)-MP-8 at pH 8 and 9.1 and for Mn(III)MP-8 at pH 10.2 and

(4) (a) Dolphin, D.; Forman, A.; Borg, D. C.; Fajer, J.; Felton, R. H. *Proc. Natl. Acad. Sci. U.S.A.* **1971**, *68*, 614−618. (b) Rutter, R.; Valentine, M.; Hendrich, M. P.; Hager, L. P.; Debrunner, P. G. *Biochemistry* **1983**, *22*, 4769−4774. (c) Pond, A. E.; Bruce, G. S.; English, A. M.; Sono, M.; Dawson, J. H. *Inorg. Chim. Acta* **1998**, *275*−*276*, 250−255.

(5) (a) Chance, B. *Arch. Biochem. Biophys.* **1952**, *41*, 416−424. (b) Dunford, H. H. In *Peroxidases in Chemistry and Biology*; Everse, J., Everse, K. E., Grisham, M. B., Eds; CRC Press: Boca Raton, FL, 1991; Vol. II, pp 1−24.

(6) (a) Baek, H. K.; van Wart, H. E. *Biochemistry* **1989**, *28*, 5714−5719. (b) Baek, H. K.; van Wart, H. E. *J. Am. Chem. Soc.* **1992**, *114*, 718−725.

(7) (a) Rodriguez-Lopez, J. N.; Smith, A. T.; Thorneley, R. N. F. *J. Biol. Chem.* **1996**, *271*, 4023−4030.

(8) (a) Dorovska-Taran, V.; Posthumus, M. A.; Boeren, S.; Boersma, M. G.; Teunis, C. J.; Rietjens, I. M. C. M.; Veeger, C. *Eur. J. Biochem.* **1998**, *253*, 659−668. (b) van Haandel, M. J. H.; Primus, J.-L.; Teunis, K.; Boersma, M. G.; Osman, A. M.; Veeger, C.; Rietjens, I. M. C. M. *Inorg. Chim. Acta* **1998**, *275*−*276*, 98−105.

(9) Coon, M. J.; Vaz, A. D. N.; Mcginnity, D. F.; Peng, H.-M. *Drug Metab. Dispos.* **1998**, *26*, 1190−1193.

(10) (a) Groves, J. T.; Watanabe, Y. *J. Am. Chem. Soc.* **1988**, *110*, 8443−8452. (b) Bell, S. E. J.; Cooke, P. R.; Inchley, P.; Leanord, D. R.; Lindsay Smith, J. R.; Robbins, A. *J. Chem. Soc., Perkin Trans. 2* **1991**, 549−559. (c) Meunier, B. *Chem. Rev.* **1992**, *92*, 1411−1456. (d) Groves, J. T.; Gross, Z.; Stern, M. K. *Inorg. Chem.* **1994**, *33*, 5065−5072.

(11) (a) Lindsay Smith, J. R.; Balasubramanian, P. N.; Bruice, T. C. *J. Am. Chem. Soc.* **1988**, *110*, 7411−7418. (b) Murata, K.; Panicucci, R.; Gopinath, E.; Bruice, T. C. *J. Am. Chem. Soc.* **1990**, *112*, 6072−6083. (c) Arasasingham, R. D.; Bruice, T. C. *J. Am. Chem. Soc.* **1991**, *113*, 6095−6103.

(12) Uno, T.; Takeda, A.; Shimabayashi, S. *Inorg. Chem.* **1995**, *34*, 1599−1607.

(13) Aron, J.; Baldwin, D. A.; Marques, H. M.; Pratt; J. M.; Adams, P. A. *J. Inorg. Biochem.* **1986**, *27*, 227−243.

(14) Osman, A. M.; Koerts, J.; Boersma, M. G.; Boeren, S.; Veeger, C.; Rietjens, I. M. C. M. *Eur. J. Biochem.* **1996**, *240*, 232−238 and references therein.

(15) Low, D. W.; Abedin, S.; Yang, G.; Winkler, J. R.; Gray, H. B. *Inorg. Chem.* **1998**, *37*, 1841−1843.

(16) Primus, J.-L.; Boersma, M. G.; Mandon, D.; Boeren, S.; Veeger, C.; Weiss, R.; Rietjens, I. M. C. M. *J. Biol. Inorg. Chem.* **1999**, *4*, 274−283.

(17) Clore, G. M.; Hollaway, M. R.; Orengo, C.; Peterson, J.; Wilson, M. T. *Inorg. Chim. Acta* **1981**, *56*, 143−148.

(18) Low, D. W.; Winkler, J. R.; Gray, H. B. *J. Am. Chem. Soc.* **1996**, *118*, 117−120.

(19) (a) Wang, J.-S.; Baek, H. K.; Van Wart, H. E. *Biochem. Biophys. Res. Commun.* **1991**, *179*, 1320−1324. (b) Osman, A. M.; Boeren, S.; Boersma, M. G.; Veeger, C.; Rietjens I. M.C. M. *Proc. Natl. Acad. Sci.* **1997**, *94*, 4295−4299.

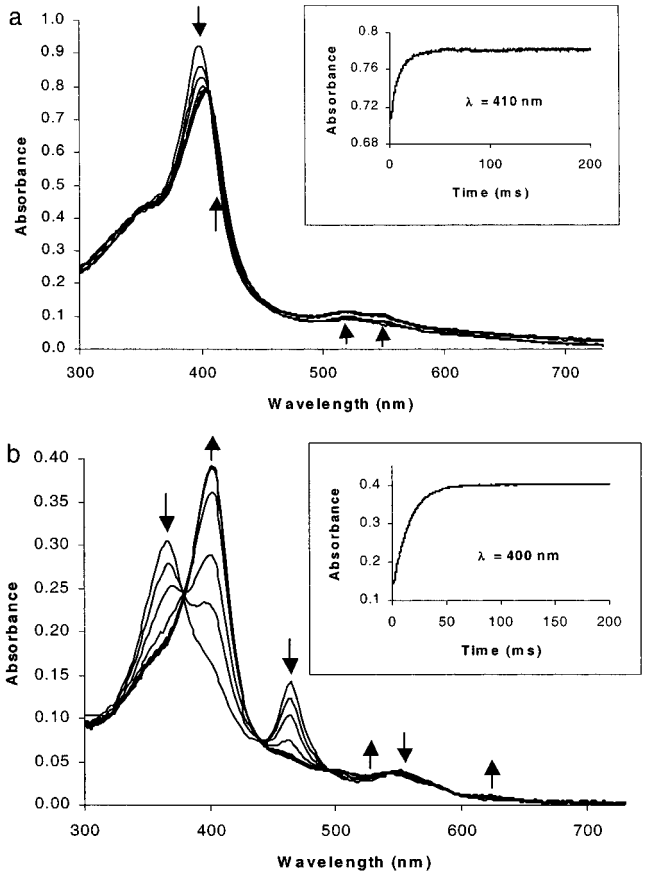

Figure 1. Time-resolved UV−visible spectra of the reaction of (a) 13.1 μM Fe(III)MP-8 with 1 mM H_2O_2 at pH 9.1 (100 scans in 300 ms, 3-ms integration time for the photodiode array; scans shown correspond to 1.3 ms, 6.4 ms, 11.5 ms, 24.3 ms, and further every tenth scan is shown for clarity); in the inset, a single-wavelength transient absorption spectra of 13.1 μM Fe(III)MP-8 mixed with 1 mM H_2O_2 at pH 9.1 is shown. Typically, 1000 data points were acquired at $\lambda = 410$ nm. Time-resolved UV−visible spectra of the reaction of (b) 8 μM Mn(III)MP-8 with 2.5 mM H_2O_2 at pH 10.9 (100 scans in 300 ms, 3-ms integration time for the photodiode array; scans shown correspond to 1.3 ms, 6.4 ms, 11.5 ms, 24.3 ms, and further every tenth scan is shown for clarity); in the inset, a single-wavelength transient absorption spectra of 6.0 μM Mn(III)MP-8 mixed with 2.5 mM of H_2O_2 at pH 10.9 is shown. Arrows indicate the time-dependent directions for the spectral variations of both Fe(III)MP-8 and Mn(III)MP-8 samples.

10.9 were plotted as function of $[H_2O_2]$. The variations of the pseudo-first-order rate constant k_{obs2} for Fe(III)MP-8 at pH 9.1 and for Mn(III)MP-8 at pH 10.2 were also plotted as function of $[H_2O_2]$. The plots of k_{obs1} as function of $[H_2O_2]$ were fitted with a rectangular hyperbola in agreement with saturation kinetics for both catalysts (Figure 2a and 2c). The values of k_{obs2} at pH 8 and 9.1 for Fe(III)MP-8 and pH 10.2 and 10.9 for Mn(III)MP-8 were found to be independent of $[H_2O_2]$ for both catalysts (see Table S3 in Supporting Information).

The double reciprocal plots of $1/k_{obs1}$ as function of $1/[H_2O_2]$ show that the data can be fitted with a linear equation for the oxidation of Fe(III)MP-8 at pH 8 and 9.1 (Figure 2b) and for the oxidation of Mn(III)MP-8 at pH 10.2 and 10.9 (Figure 2d). The fact that, for both catalysts, the linear fits of $1/k_{obs1}$ at different pH values have a different slope but a common intercept on the vertical axis indicates a competitive role played by protons in the formation of the oxidized species of M(III)-MP-8.

The effect of the protons was further confirmed by studying the variation of k_{obs1} as function of the proton concentration

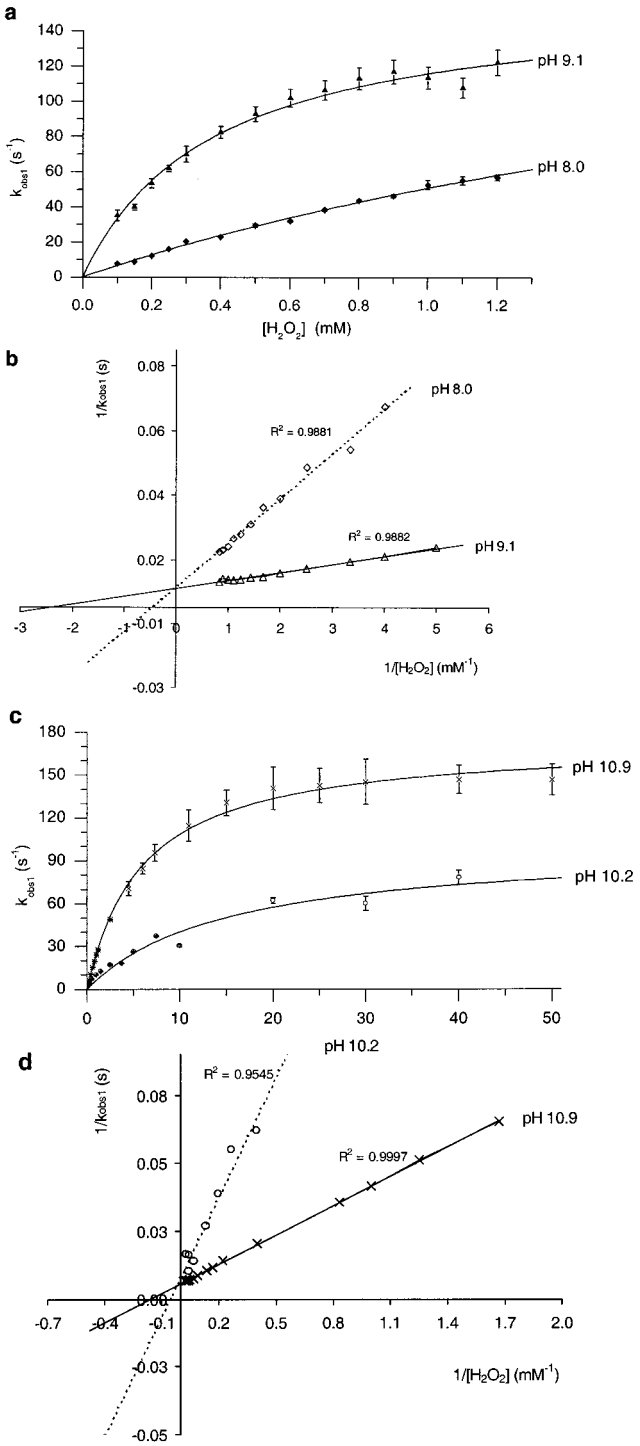

Figure 2. Variation of the pseudo-first-order rate constant of the first step k_{obs1} for (a) Fe(III)MP-8 at pH 8.0 and 9.1 and for (c) Mn(III)MP-8 at pH 10.2 and 10.9 as a function of $[H_2O_2]$; (b) and (d) are the double reciprocal plots of respectively (a) and (c). For both Fe(III)MP-8 and Mn(III)MP-8, the values of k_{obs1} follow saturation kinetics, and least-squares linear fitting of the data in (b) and (d) reveals a competitive role played by protons in the reaction of M(III)MP-8 with H_2O_2, error bars were omitted for clarity. [Fe(III)MP-8] = 8.7 μM at pH 9.1; 13.1 μM at pH 8.0 and [Mn(III)MP-8] = 6.0 μM at pH 10.9; 7.9 μM at pH 10.2.

for a specific hydrogen peroxide concentration. The pH was varied from pH 8 to pH 10, using a series of complementary buffers, for Fe(III)MP-8 in the presence of 1 mM H_2O_2; the pH was varied from pH 9.9 to pH 13 for Mn(III)MP-8 in the presence of 2.5 mM H_2O_2. The values of $1/k_{obs1}$ as function of

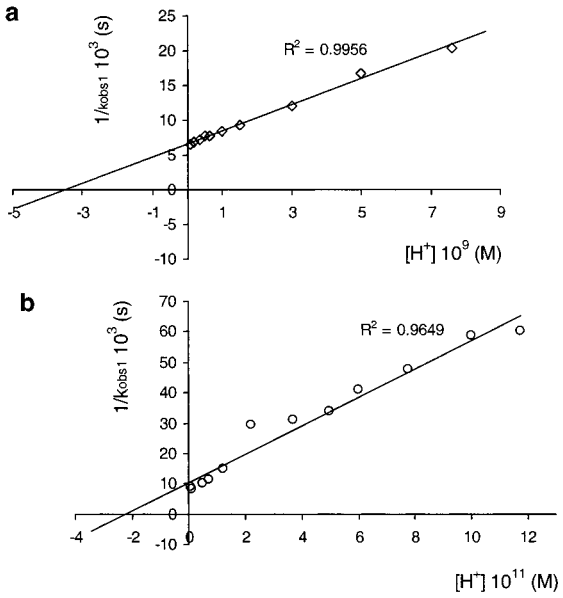

Figure 3. Variations of $1/k_{obs1}$ as function of $[H^+]$ for (a) [Fe(III)MP-8] = 8.7 μM; $[H_2O_2]$ = 1 mM and for (b) [Mn(III)MP-8] = 7.9 μM; $[H_2O_2]$ = 2.5 mM showing that k_{obs1} increases at higher pH values. Data were fitted with a linear least-squares procedure, error bars were omitted for clarity.

$[H^+]$ could be fitted with a linear equation (Figure 3a and 3b). For both catalysts, the values of k_{obs1} are shown to increase with the pH. The variations of k_{obs2} in the presence of 1 mM H_2O_2 for Fe(III)MP-8 and in the presence of 2.5 mM H_2O_2 for Mn(III)MP-8 were plotted as function of $[H^+]$ and were found to be independent of $[H^+]$ (see Table S3 in Supporting Information). Observed rate constants of $k_{obs2} = 13.1 \pm 1.0$ s^{-1} and $k_{obs2} = 5.2 \pm 1.2$ s^{-1} were measured for Fe(III)MP-8 and Mn(III)MP-8, respectively.

The UV−visible spectra of the resting state of the catalysts show a Soret band at 396 nm and Q-bands at 510 and 623 nm for Fe(III)MP-8 (Figure 1a)[18] and a split Soret band at 368 and 460 nm with Q-band at 552 nm for Mn(III)MP-8 (Figure 1b).[15] Simulations of the reaction of Fe(III)MP-8 with H_2O_2 show the spectrum of the final product of the first exponential step (k_{obs1}) to be typical of a high-valent iron-oxo intermediate, Fe(IV)-MP-8=O, isoelectronic to a peroxidase Compound II species (see also Figure 1a). The spectrum depicts a red-shifted Soret band at 406 nm and characteristic Q-bands at 519 and 548 nm.[18,19a] For the reaction of Mn(III)MP-8, with H_2O_2, simulations of the spectrum of the final product of the first exponential step (k_{obs1}) show a spectrum typical of a high-valent manganese-oxo intermediate, Mn(IV)MP-8=O, having a strong Soret band at 401 nm and shifted Q-bands at 541 and 623 nm (see also Figure 1b).[15,20] Figure 4a depicts the X-band transient EPR spectra of Mn(III)MP-8 incubated with an excess of H_2O_2 at pH 11.5. The occurrence of a broad moderate resonance at $g \approx 4$ is compatible with a high spin (S =3/2) monomeric Mn(IV), the species as shown by the spectrum simulation. This species could be assigned to a high-valent manganese-oxo intermediate.[20,21] A free radical signal at $g = 2.00$ is also detected,

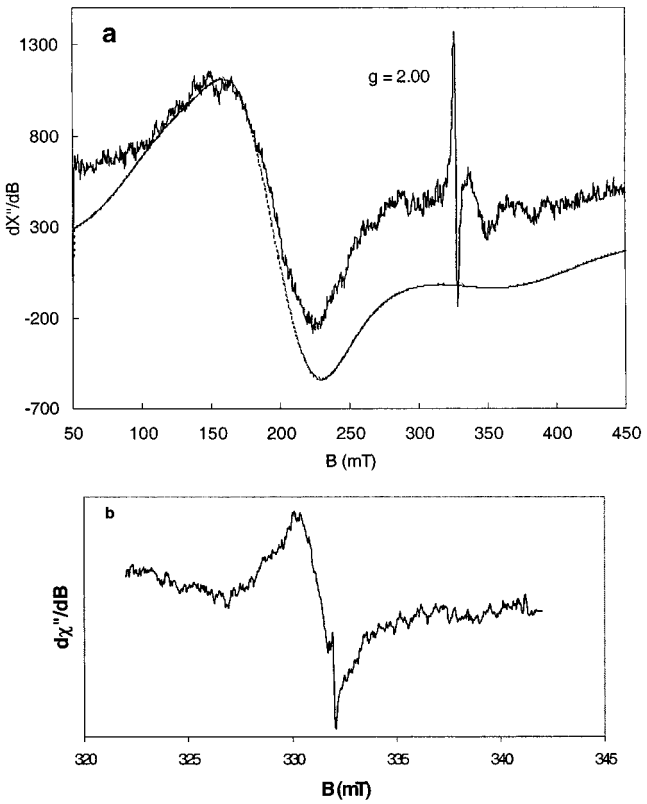

Figure 4. (a) Transient spectrum of 1 mM Mn(III)MP-8 incubated with 25-fold excess of H_2O_2 in 0.1 M carbonate pH 11.5 and simulated trace (smooth line) for a Mn(IV) (S =3/2) system; $E/D \approx 0.1$. A resonance assigned to a Mn(IV) (S = 3/2) species is visible at $g \approx 4$ and a free radical signal is indicated at $g \approx 2.00$. EPR conditions: microwave frequency 9.227 GHz, microwave power 12.6 mW, modulation frequency 100 kHz, modulation amplitude 1 mT, temperature 16 K. (b) Transient spectrum of the free radical observed after treatment of 1 mM Mn(III)MP-8 with 25-fold excess of H_2O_2 in 0.1 M carbonate pH 11.5. EPR conditions: microwave frequency 9.227 GHz, microwave power 20 mW, modulation frequency 100 kHz, modulation amplitude 0.125 mT, temperature 45 K.

suggesting the formation of a protein radical on the peptide part of Mn(III)MP-8 concomitantly with the Mn(IV)MP-8=O species. Figure 4b depicts the radical signal showing a bandwidth of approximately 9 mT. The hyperfine splitting observed ($A \approx$ 1.5 mT) suggests a coupling of the free radical electron with a neighboring nucleus. Figure 5 presents the microwave power saturation plots of the free radical signal at 43 and 50 K.

Discussion

Kinetic Analysis. The present study describes rapid kinetics for the formation of oxidized Fe(III)MP-8 and Mn(III)MP-8 upon reaction with H_2O_2 as function of $[H^+]$. The system is experimentally described by two observed monoexponential steps (k_{obs1} and k_{obs2}) for Fe(III)MP-8 and Mn(III)MP-8 pointing at the fact that there is an intermediate C which is formed between the two steps. The analysis of the data, for the first observed monoexponential step k_{obs1}, is based on the following reaction sequence which shows one nonreversible elementary step preceded by two reversible elementary steps (see later for justification) (Scheme 1).

The observation of saturation kinetics for both Fe(III)MP-8 and Mn(III)MP-8 (Figure 2) strongly suggests the formation of an intermediate B during the observed step k_{obs1}. Also, inspection of the saturation plots indicates that the conversion of B to C is

(20) Ayougou, K.; Bill, E.; Charnock, J. M.; Garner, C. D.; Mandon, D.; Trautwein, A. X.; Weiss, R.; Winkler, H. *Angew. Chem., Int. Ed. Engl.* **1995**, *34*, 343−346.
(21) Czernuszewicz, R. S.; Su, O. Y.; Stern, M. K.; Macor, K. A.; Kim, D.; Groves, J. T.; Spiro, T. G. *J. Am. Chem. Soc.* **1988**, *110*, 4158−4165.

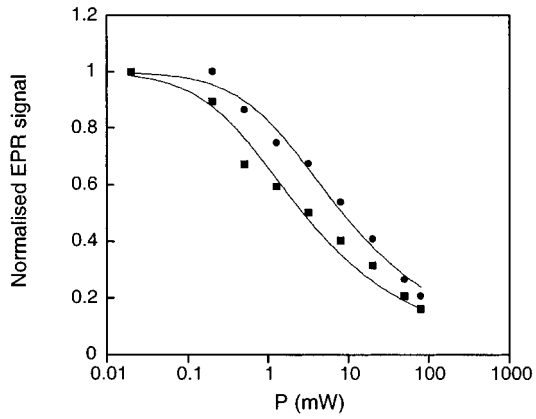

Figure 5. EPR microwave power-saturation behavior of the free radical signal of MnMP-8. Half-saturation power were respectively obtained at $T = 43$ K, $P_{1/2} = 0.44 \pm 0.06$ mW (■) and $T = 50$ K, $P_{1/2} = 1.36 \pm 0.13$ mW (●). Data were fitted according to eq 9.

Scheme 1

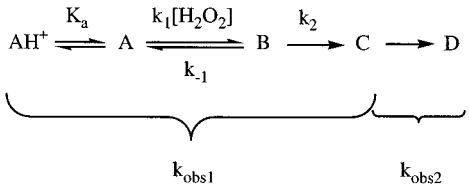

a nonreversible process. Finally, the competitive effect of the protons observed during the first step k_{obs1} (Figure 3) can be interpreted as the deprotonation step of a protonated precursor of A, denoted AH^+.

Considering the mechanism depicted in Scheme 1, the rate of formation of B can be written as follows:

$$\frac{d[B]}{dt} = k_1[H_2O_2][A] - k_2[B] - k_{-1}[B] \qquad (1)$$

also,

$$[A]_{tot} = [AH^+] + [A] + [B] \qquad (2)$$

and

$$K_a = \frac{[A][H^+]}{[AH^+]} \qquad (3)$$

Combining (2) and (3), substituting in (1), and assuming a steady-state regime for the formation of B lead to:

$$[B] = \frac{[H_2O_2][A]_{tot}}{\left(1 + \frac{[H^+]}{K_a}\right)\left(\frac{k_{-1} + k_2}{k_1}\right) + [H_2O_2]} \qquad (4)$$

Using the following rate law to describe the formation of C in Scheme 1:

$$v = \frac{d[C]}{dt} = k_{obs1}[A]_{tot} = k_2[B] \qquad (5)$$

a hyperbolic equation for k_{obs1} is consecutively obtained:

$$k_{obs1} = \frac{k_2[H_2O_2]}{\left(1 + \frac{[H^+]}{K_a}\right)\left(\frac{k_{-1} + k_2}{k_1}\right) + [H_2O_2]} \qquad (6)$$

Using the double reciprocal form of eq 6, the values of the first-order rate constant k_2 could be calculated from the double reciprocal plots of Figure 2. Consequently, $k_2 = 165 \pm 8$ s^{-1} for Fe(III)MP-8 and $k_2 = 145 \pm 7$ s^{-1} for Mn(III)MP-8 (from Figure 2b and 2d, respectively). From the value of k_2 for Fe(III)-MP-8, it can be derived that approaching the conversion of B into C by an irreversible step is justified by the fact that, also in view of the oxygen exchange between H_2O_2 and water, the total reaction is reversible,[8a,b] but with a reverse rate k_{-2} estimated at 0.03 M^{-1}s^{-1},[8b] more than 2 orders of magnitude smaller than k_2.

When $[H_2O_2]$ is kept constant, eq 6 can be rewritten as follows:

$$\frac{1}{k_{obs1}} = \frac{1}{k'_{obs1}} + \frac{1}{k_2} + \frac{[H^+]}{K_a k'_{obs1}} \qquad (7)$$

where k'_{obs1} is a theoretical pseudo-first-order rate constant independent of the protons and dependent on $[H_2O_2]$. As proposed in the results section, the plots of Figures 2 and 3 point at a competitive effect of the protons for the formation of intermediate B. The inhibition constant K_a is calculated from the plots of Figure 3 using eq 7 and gives $pK_a = 9.6 \pm 0.5$ for Fe(III)MP-8 and $pK_a = 11.1 \pm 0.5$ for Mn(III)MP-8. Both values are in good agreement with the pH optimum values for respectively Fe(III)MP-8 and Mn(III)MP-8 supported peroxidase catalysis and Fe(III)MP-8 supported P450-catalysis.[16] The pK_a values can also be calculated from the double reciprocal plots of Figure 2b and 2d using the double reciprocal form of eq 6. The values calculated are $pK_a = 8.9 \pm 0.5$ for Fe(III)MP-8 and $pK_a = 11.4 \pm 0.5$ for Mn(III)MP-8 in agreement with the ones obtained from Figure 3.

At low $[H_2O_2]$ and assuming $k_{-1} \ll k_2$, eq 6 becomes:

$$k_{obs1} = \frac{k_1[H_2O_2]}{\left(1 + \frac{[H^+]}{K_a}\right)} \qquad (8)$$

The second-order rate constant k_1 can be determined from the tangent of the initial slope of the $[H_2O_2]$-saturation plots in Figure 2a and 2c using eq 8. For Fe(III)MP-8, $k_1 = (1.1 \pm 0.1) \times 10^6$ M^{-1}•s^{-1} at pH 8 and $k_1 = (1.2 \pm 0.1) \times 10^6$ M^{-1}•s^{-1} at pH 9.1; for Mn(III)MP-8, $k_1 = (2.0 \pm 0.2) \times 10^5$ M^{-1}•s^{-1} at pH 10.2 and $k_1 = (1.2 \pm 0.1) \times 10^5$ M^{-1}•s^{-1} at pH 10.9. Consecutively, using the double reciprocal form of eq 6, k_{-1} can be determined from the plots of Figure 2b and 2d. For Fe(III)MP-8, $k_{-1} = 0.8 \pm 0.08$ s^{-1} at pH 8 and $k_{-1} = 14.3 \pm 1.4$ s^{-1} at pH 9.1; for Mn(III)MP-8, $k_{-1} = 9.6 \pm 1.0$ s^{-1} at pH 10.2 and $k_{-1} = 31.8 \pm 3.2$ s^{-1} at pH 10.9. The obtained values of k_{-1} confirm that the assumption made for deriving eq 8 is correct. Moreover, with $k_{-1} \ll k'_1$ (see equation A3) the rate constant k_{-1} can be ignored in Scheme 1 and it becomes possible to simulate the first step of the transient kinetics traces, k_{obs1}, using an equation describing the variation of [C] as function of time (eq A1). The value of k_1 can be determined from the simulation with good confidence, considering that the time-

Table 1. Mean Values of the Kinetic and Thermodynamic Constants Determined in This Study, for the Reaction of H_2O_2 with Fe(III)MP-8 and Mn(III)MP-8[a]

	$pK_a \pm 3\sigma$[b]	$k_1 \pm 3\sigma$ ($M^{-1}\cdot s^{-1}$)[c]	$k_{-1} \pm 2\sigma$ (s^{-1})	k_2 (s^{-1})	k_{-2} ($M^{-1}\cdot s^{-1}$)	k_{obs2} (s^{-1})
Fe(III)MP-8	9.2 ± 0.9	$(1.3 \pm 0.6) \times 10^6$	7.5 ± 12	165 ± 8	0.03 ± 0.01[d]	13.1 ± 1.1
Mn(III)MP-8	11.2 ± 0.3	$(1.6 \pm 0.9)\ 10^5$	20.7 ± 11	145 ± 7	nd	5.2 ± 1.2

[a] The pK_a corresponds to the deprotonation of metal-bound water for both catalysts, k_1 to the second-order rate constant for the formation of M(III)MP-8-OOH, k_{-1} to the corresponding first-order reverse rate constant, k_2 to the first-order rate constant for the cleavage of M(III)MP-8-OOH, and k_{-2} to the corresponding reverse second-order rate constant. The pseudo-first-order rate constant k_{obs2} corresponds to the decaying phase of the postulated high-valent metal-oxo peptide radical intermediate. See Discussion for the calculation of these parameters. [b] The mean pK_a value was used to calculate k_1 and k_{-1}. [c] The mean value of k_1 was used to calculate k_{-1}. [d] Calculated from van Haandel et al..[8b]

dependent transient absorbance changes, recorded at 410 nm for Fe(III)MP-8 and 400 nm for MnMP-8, almost exclusively account for the formation of C. Simulation of selected traces gives for Fe(III)MP-8, $k_1 = (1.6 \pm 0.2) \times 10^6\ M^{-1}\cdot s^{-1}$ and for Mn(III)MP-8, $k_1 = (1.6 \pm 0.2) \times 10^5\ M^{-1}\cdot s^{-1}$. The good agreement of these values with the ones estimated from the saturation plots of Figure 2 again confirms that the assumption of ignoring k_{-1} for determining k_1 using eq 8 is correct. The average values of the kinetics and thermodynamic parameters obtained for both catalysts are given in Table 1. From this table it can also be noticed that the rate constants determined in this study are higher than the value of $k \sim 0.1\ s^{-1}$ assigned to the oxidative degradation of MP-8 by 2.5 mM H_2O_2 as obtained by Spee et al.,[22] thereby confirming that degradation processes of the catalyst can be ignored for the understanding of the present kinetic analysis.

Nature of the Intermediates. The determination of the nature of the different intermediates A, B, C, and D is based on the following facts. (i) The transient UV−visible spectra of C and D are similar (see Figure 1) and can be assigned to a high-valent metal-oxo MP-8 species; (ii) The transient EPR of Mn(III)MP-8 reacted with H_2O_2 during 27 ms indicates that a free radical species is formed concomitantly to a high-valent manganese-oxo species. (iii) The conversion of C into D is independent of $[H^+]$ and $[H_2O_2]$; (iv) The conversion of B into C is rate-limiting, except at very low $[H_2O_2]$, and leads to the accumulation of B; (v) The observed rate of formation of C increases at higher pH values.

In consequence, two species, C and D, depict the same UV−visible fingerprint but are kinetically well defined as two separated intermediates. For MnMP-8, using equation (A1), a calculation of the concentration of C after 27 ms reaction time in the conditions of the EPR measurement shows that the reaction mixture should mainly contain 65% of intermediate C. A tentative assignment for C could be a possible high-valent manganese-oxo MP-8 with a free radical species not located on the porphyrin macrocycle. Intermediate D would represent the decaying species of C with no more free radical character but still regarded as a high-valent manganese-oxo species on the basis of the UV−visible spectra. For the reaction of Fe(III)-MP-8 with H_2O_2, there is no evidence of a free radical character on the peptide of the molecule for intermediate C. However, the mechanism of oxidation common to Mn(III)MP-8 and Fe(III)MP-8 suggests an assignment, similar to the one made for Mn(III)MP-8, for intermediates C and D of Fe(III)MP-8. Moreover, the formation of intermediate C follows saturation kinetics. Consequently, intermediate B can be assigned to the

Scheme 2

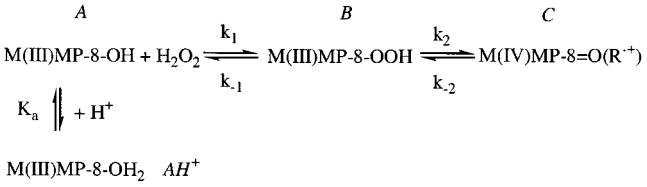

Compound 0 of MP-8, M(III)MP-8-OOH.[6a,19a] In the reaction cycle of peroxidases, Compound 0 is preceding the formation of an intermediate consisting of a high-valent iron-oxo species and a radical species. A reasonable structure for intermediate C would therefore be a high-valent metal-oxo MP-8 peptide radical, M(IV)MP-8=O($R^{\bullet+}$), and for intermediate D a high-valent metal-oxo MP-8, M(IV)MP-8=O. Recently, on the basis of rapid-freeze EPR and Mössbauer spectroscopy, such a structure has been proposed for the peroxy acetic acid oxidized product of cytochrome $P450_{cam}$ of which the accompanying radical is proposed to be localized on a tyrosine residue localized in the proximal heme active site.[23] For Mn(III)MP-8, one may speculate on which residue the free radical is localized. The most likely candidate is, in view of the hyperfine splitting and the fact that MP-8 does not contain any aromatic amino acids, the histidine ligand.

Finally, the pK_a value measured in this study for Fe(III)MP-8 is found in good agreement with the pK_a of Fe(III)MP-8 iron bound water deprotonation ($pK_a = 9.6$).[24a,b] The two units higher pK_a value measured for Mn(III)MP-8 (Table 1) is consistent with the lower reduction potential of the manganese catalyst[16] and can be assigned to manganese-bound water deprotonation. The rapid deprotonation of the aquo ligand is a prerequisite to form a species, M(III)MP-8-OH (intermediate A), able to react with H_2O_2 and to form Compound 0. The second-order rate constant for the reaction of Fe(III)MP-8-OH with H_2O_2, $k_1 = 1.3 \times 10^6\ M^{-1}\cdot s^{-1}$, is about 8 times higher than the corresponding rate constant for Mn(III)MP-8-OH, $k_1 = 1.6 \times 10^5\ M^{-1}\cdot s^{-1}$. The value of k_1 found for the iron system is roughly 7-fold lower than the one found by Chance for HRP ($k_1 = 9 \times 10^6\ M^{-1}\cdot s^{-1}$).[5a,25] The first-order rate constant for heterolytic cleavage of Fe(III)MP-8-OOH, $k_2 = 165\ s^{-1}$, is found slightly higher than for Mn(III)MP-8-OOH, $k_2 = 145\ s^{-1}$, suggesting that the nature of the metal does not play a significant role for the heterolytic cleavage step.

In conclusion, the reaction sequence describing k_{obs1} in Scheme 1 can now be written in the following way (Scheme 2; intermediates AH^+, A, B, and C are indicated in italics).

(22) Spee, J. H.; Boersma, M. G.; Veeger, C.; Samyn, B.; van Beeumen, J.; Warmerdam, G.; Canters, G. W.; van Dongen, W. M. A. M.; Rietjens, I. M. C. M. *Eur. J. Biochem.* **1996**, 241, 215−220.

(23) Schünemann, V.; Jung, C.; Trautwein, A. X.; Mandon, D.; Weiss, R. *FEBS Lett.* **2000**, 179, 149−154.

(24) (a) Baldwin, D. A.; Marques, H. M.; Pratt, J. M. *J. Inorg. Biochem.* **1986**, *27*, 245−254. (b) Wang, J.−S.; Tsai, A.-L.; Heldt, J.; Palmer, G.; van Wart, H. E. *J. Biol. Chem.* **1992**, *267*, 15310−15318.

Conclusion

This study provides a comprehensive explanation for the pH-dependent reactivity of Fe(III)MP-8 and Mn(III)MP-8 with H_2O_2. The absence of a real active site pocket for MP-8, with a distal basic residue participating in the peroxide deprotonation and favoring the O−O peroxide bond cleavage, could somehow be responsible for the low reactivity of MP-8 at low pH when compared to HRP. Increase of the pH induces metal-bound water deprotonation, which subsequently, either assists concerted hydrogen peroxide deprotonation and coordination of the hydroperoxo group to the metal center or is directly oxidized by hydrogen peroxide into a metal-hydroperoxo MP-8. For HRP, His42 could deprotonate the iron-bound water and promote a similar mechanism as the one suggested for MP-8. Compound 0 is subsequently converted into what can best be described as a high-valent metal-oxo intermediate and a peptide free radical. This latter intermediate slowly decays into a high-valent metal-oxo species.

Experimental Section

Chemicals. Cytochrome *c* from horse heart was obtained from Boehringer (Mannheim, Germany). Fe(III)MP-8 was prepared by proteolytic digestion of horse heart cytochrome *c* essentially as described previously.[13,18] Anhydrous iron(II) chloride was obtained from Strem Chemicals (Newburyport MA). Manganese(II) sulfate tetrahydrate, L-ascorbic acid, and H_2O_2 30% v/v were from Merck (Darmstadt, Germany). The concentration of the diluted H_2O_2 solutions was always checked spectrophotometrically using the molar extinction coefficient at 240 nm, $\epsilon_{240} = 39.4 \pm 0.2\ M^{-1}\cdot cm^{-1}$.[27] All water solutions were prepared with deionized or Nanopure water (mixed bed of ion exchanger, Millipore) and the pH was measured using a combined glass microelectrode (Ingold, High Alcalinity). The reference electrode (Ag/AgCl) was filled with a saturated solution of NaCl (Merck, Darmstadt, Germany) containing traces of silver chloride (Merck, Darmstadt, Germany) and the pH meter was calibrated using buffer solutions (Prolabo, Normadose). All HPLC solvents were of chromatographic grade. All others reagents used were of analytical grade.

Synthesis of Mn(III)MP8. Manganese substituted MP-8 was prepared by metalation of MP-8 free base. Demetalation was essentially performed using an improved published method.[16] During all the preparation, the reaction medium was protected from light. A solution of Fe(III)MP-8 (206 mg, 137 μmol) in 200 mL of ice cold acetic acid was made oxygen free by three cycles of vacuum/argon; 410 μL of a 0.5 mg/mL argon saturated $Fe(II)Cl_2$ water solution (12-fold excess, 1.64 mmol) were introduced together with 1.7 mL 36% aqueous HCl (100 mM). Another three cycles of vacuum/argon was applied to the reaction mixture before it was allowed to stir for 5 min at ambient temperature in a light-protected glass bottle. The reaction mixture was first evaporated (20 mmHg/40 °C) to dryness, washed with water, and re-evaporated to dryness (20 mmHg/40 °C). The demetalated material was dissolved in a minimal volume of 0.05 M ammonium hydrogenocarbonate pH 7 and loaded on a Sephadex LH-20 column eluted with MeOH at 0.2 mL/min. Fractions free from iron salts were pooled and evaporated to dryness (20 mmHg/40 °C). The remaining red material stuck to the column was discarded by washing with MeOH/AcOH/H_2O: 5/1/4.

Metalation was essentially performed using an adapted literature procedure.[15] The demetalated material was dissolved in 60 mL of 0.05 M ammonium acetate pH 5.5 giving a roughly 1−2 mM concentrated solution. The solution was saturated with argon by three cycles of vacuum/argon and 135 mg of $Mn(II)SO_4$ tetraydrate (600 μmol) were added to the reaction mixture which was stirred at 40 °C in a light-protected glass bottle. After 37 h, another 135 mg of $Mn(II)SO_4$ tetrahydrate (600 μmol) was added to the reaction mixture which was made argon saturated by three cycles of vacuum/argon. The amount of Mn(III)MP-8 formed was regularly checked by HPLC. Usually after about 60 h of reaction, the mixture contained 90% Mn(III)MP-8 and 10% MP-8 free base determined by UV detection at 220 nm. The reaction was stopped at that point and the mixture subsequently concentrated and washed to remove inorganic salts using an Amicon ultra-filtration cell with a YC05 membrane. The metalated material was further purified by semipreparative HPLC.

Purification of crude Mn(III)MP8 was performed using two Isco Model 2300 HPLC pumps equipped with a Pye Unicam LC−UV Detector. The Mn(III)MP-8 solution was filtered and the filtrate, typically 5 mL, was loaded on a Waters Delta-Pak C18 column (25 mm × 200 mm, 300 Å pore size, 10 μm particle size). Elution was performed with a gradient of TEAP pH 7 (eluent A) and CH_3CN (eluent B).[16] For semipreparative purification of the intermediate, 26% of B was first applied for 3 min and simultaneously the flow was increased from 4 $mL\cdot min^{-1}$ to 8 $mL\cdot min^{-1}$. Elution was achieved by applying a linear gradient of B from 26% to 37% over 11 min followed by further increase to 41% within 30 s at 8 $mL\cdot min^{-1}$. The collected fractions were pooled, concentrated by evaporation (20 mmHg, 35 °C), and finally lyophilised. Mn(III)MP-8 was checked for purity on analytical HPLC and dialyzed against a 10 mM pH 9 carbonate buffer.

Stopped-Flow Measurements. Solutions of Fe(III)MP-8 and corresponding H_2O_2 solutions were both buffered with either 0.1 M potassium phosphate (pH 8.0), 0.1 M tricine (from pH 8.1 till pH 9), or 0.1 M potassium carbonate (from pH 9.1 till pH 10). For Fe(III)-MP-8, concentrations of the oxygen donor, H_2O_2, were varied between 0.1 mM and 1.2 mM. Concentrations of Fe(III)MP-8 were chosen between 8.7 μM and 13.1 μM and were calculated using $\epsilon_{397} = 1.57 \times 10^5\ M^{-1}\cdot cm^{-1}$ for Fe(III)MP-8 at pH 7.[13] Solutions of Mn(III)MP-8 and corresponding H_2O_2 solutions were both buffered with either 0.1 M potassium carbonate (from pH 10 till pH 11) or 0.1 M potassium phosphate (from pH 11.1 till pH 13). For the manganese complex, Mn(III)MP-8, concentrations of the oxygen donor, H_2O_2, were varied between 0.6 mM and 50 mM. Concentrations of Mn(III)MP-8 were chosen between 6 μM and 7.9 μM and were calculated using the value of ϵ_{463} determined to be $2.82 \times 10^4 \pm 3.36 \times 10^3\ M^{-1}\cdot cm^{-1}$ for Mn(III)-MP-8 at pH 7. Indicated concentrations are the final concentrations after mixing. All measurements were performed under pseudo-first-order conditions with at least a 10-fold excess of H_2O_2 with respect to [Fe(III)MP-8] or [Mn(III)MP-8] and at a thermostated temperature of 25 ± 0.2 °C. Kinetic and thermodynamic constants are presented with 98% or 95% confidence, respectively $x \pm 3\sigma$ and $x \pm 2\sigma$.

Time-resolved spectra were recorded on an Applied Photophysics SX-18 MV stopped-flow spectrophotometer (Leatherhead, UK) using the photodiode array rapid-scan mode. The spectral resolution was around 1 nm with a mixing time of 3 ms. For the current study, no spectral information was lost during the mixing time. Reaction profiles were collected in the monochromatic mode of an Applied Photophysics (Leatherhead, UK) stopped-flow spectrophotometer. No kinetic information was lost during the 3 ms mixing time and currently 1000 data points per trace were acquired. The length of the light path was 1 cm for both types of measurements. The data sets, average out of three independent measurements, were recorded at 410 nm for Fe(III)MP-8[18] and 400 nm for Mn(III)MP-8[15], both strong absorbances in the spectrum of the oxidized products. Traces were processed online with commercial softwares based on the Marquardt algorithm (SpectraKinetic Software, Applied Photophysics Ltd., Leatherhead UK 1992) or on the Simplex algorithm (Biokine v. 3.14, Bio-logic Co, Echirolles France 1991). Time-resolved spectra were simulated using a commercial software based on the Marquardt algorithm (Specfit Global Analysis v.2.11, Rev.C, Spectrum Software Associates, Chapel Hill NC 1993).

(25) Chance, B. *J. Biol. Chem.* **1943**, *151*, 553−577.
(26) Moore, J. W.; Pearson, R. G. *Kinetics and Mechanism*; John Wiley and Sons: New York, **1980**; pp 290−296.
(27) Nelson, D. P.; Kiesow, L. A. *Anal. Biochem.* **1972**, *49*, 474−478.

Simulations of transient kinetic traces to determine k_1 were done by fitting equation (A1) to the curve and taking the value of k_2 as determined from figure 2b and 2d.

Rapid-Freeze and EPR Measurements. Rapid-freeze experiments were performed on a home-built apparatus following the method described by Duyvis.[28] EPR samples were prepared by mixing solutions of 1 mM Mn(III)MP-8 in 0.1 M carbonate at pH 11.5 with a 25-fold excess of H_2O_2 in the same buffer. After mixing, solutions were incubated in the aging hose for 27 ms on the basis of the analysis performed with the stopped-flow instrument. Samples were immediately frozen by spraying them into a funnel, connected with a rubber to the EPR tube. Both the funnel and the EPR tube were immersed and filled with cold isopentane cooled with liquid nitrogen (around −140 °C). EPR experiments were performed on a Varian E−4 X-band EPR spectrometer. For Mn(III)MP-8, experiments were performed at 9.227 GHz microwave frequency with the following measurement conditions: modulation frequency 100 kHz, gain, 6.3×10^3; scan time, 4 min; time constant, 0.1 s. The center of the field was set at 250 mT; spectra were recorded over a 400 mT range and corrected for blank absorption. The microwave power at half saturation $P_{1/2}$ was calculated using the saturation curve described in the literature:[23,29]

$$I \propto (1 + P/P_{1/2})^{-b/2} \tag{9}$$

I is the EPR amplitude and P is the microwave power. The inhomogeneity parameter b was estimated to be 0.7 from the linearization of eq 9.[29] This suggests inhomogeneous broadening of the signal.

Abbreviations. M(III)MP-8-OOH, Fe(III)MP-8-OOH, or Mn(III)-MP-8-OOH: metal-, iron-, or manganese-hydroperoxo microperoxidase-8, respectively; Fe(IV)MP-8=O or Mn(IV)MP-8=O, high-valent iron- or manganese-oxo microperoxidase-8, respectively; Fe(IV)MP-8=O($R^{\bullet+}$) or Mn(IV)MP-8=O($R^{\bullet+}$): high-valent iron- or manganese-oxo peptide radical cation microperoxidase-8, respectively, (Compound ES-like); PorFe(III): iron porphyrin, the same nomenclature as for MP-8 is further used for the oxidized iron porphyrin intermediates; HRP: horseradish peroxidase, P450(s): cytochrome(s) P450. FeTDCPPS or MnTDCPPS: (meso-tetrakis-(2,6-dichloro-3-sulfonatophenyl)-porphinato)iron or manganese. ϵ_{240}: molar absorption coefficient at 240 nm.

Acknowledgment. The authors gratefully acknowledge Dr. Huub Haaker for help with the rapid-freeze experiments and Prof. Dr. R. Weiss for constant support. The EU Copernicus program (Grant No. ERBIC15-CT961004), the Dutch Foundation for Technical Research (CW/STW Project No. 349-3710), and the Centre National pour la Recherche Scientifique (CNRS, France) are also acknowledged.

Appendix

Expression of the variation of [C] as function of time for a consecutive nonreversible reaction sequence (reaction AI, below).

Ignoring k_{-1} in Scheme 1, the following consecutive nonreversible elementary two-step reaction sequence preceded by a rapid preequilibrium is used to describe k_{obs1}:

$$AH^+ \overset{K_a}{\rightleftharpoons} A \xrightarrow{k_1[H_2O_2]} B \xrightarrow{k_2} C \tag{AI}$$

The expression of the variation of [C] as function of time is adapted from Moore and Pearson[26] leading to

$$[C] = \frac{[A]_0 K_a}{(K_a + [H^+])}\left[1 + \frac{1}{(k_1' - k_2)}(k_2 \exp(-k_1' t) - k_1' \exp(-k_2 t))\right] \tag{A1}$$

with

$$[A]_0 = [A]\frac{(K_a + [H^+])}{K_a} \tag{A2}$$

and

$$k_1' = \frac{K_a k_1 [H_2O_2]}{K_a + [H^+]} \tag{A3}$$

The apparent first-order rate constant k_1' can be simulated using equation (A1), and k_1 is consecutively obtained by using equation (A3).

Supporting Information Available: Tabulated values for the pseudo-first-order rate constants of the first and the second step k_{obs1} (Table S1 and S2) and k_{obs2} (Table S3). The observed rate constants of both steps are given for Fe(III)MP-8 and Mn(III)-MP-8 as function of $[H_2O_2]$ at given pH and as function of $[H^+]$ at given $[H_2O_2]$ (PDF). This material is available free of charge via the Internet at http://pubs.acs.org.

JA016907U

(28) Duyvis, M. G. Kinetics of nitrogenase from *Azotobacter vinelandii*. Doctorate Dissertation, Wageningen University, Wageningen, The Netherlands, 1997; p 90.
(29) Sahlin, M. P.; Gräslund, A.; Ehrenberg, A. *J. Magn. Reson.* **1986**, *67*, 135−137.